

Molecular Growth of Polyoxometalate Architectures Based on $[-Ag\{Mo_8\}Ag-]$ Synthons: Toward Designed Cluster Assemblies

Hamera Abbas, Carsten Streb, Alexandra L. Pickering, Andrew R. Neil, De-Liang Long, and Leroy Cronin*

WestCHEM, Department of Chemistry, Joseph Black Building, University of Glasgow, Glasgow, G12 8QQ, U.K.

Received August 5, 2007; Revised Manuscript Received November 17, 2007

ABSTRACT: The interaction of silver(I) cations with octamolybdate $[Mo_8O_{26}]^{4-}$ has been investigated by applying the principles of the building-block concept to the well established silver–octamolybdate reaction system. The self-assembly of dimeric $\{Ag_2\}$ linkers allows the formation and isolation of chains and networks where $[Mo_8O_{26}]^{4-}$ clusters are cross-linked by silver(I) cations. The influence of the solvent on the overall topology has been studied, and the role of the counterion on the resulting structure has been highlighted in each assembly. Fine-tuning of the metal–metal distances of the dimeric $\{Ag_2\}$ linking units has been achieved by using different coordinating solvents which act as bridges. Five compounds based on silver octamolybdate building blocks have been isolated, including an uncommon intermediate $((Ph_4P)_2[Ag_2(CH_3CN)_2(Mo_8O_{26})])$, three one-dimensional polymeric chains $([Ag(C_7H_{12}O_2N)(CH_3CN)]_{2n}[Ag_2(CH_3CN)_2(Mo_8O_{26})]_n \cdot 2CH_3CN)$, $(Ph_4P)_{2n}[Ag_2(DMF)_2(Mo_8O_{26})]_n \cdot 2DMF$, and $(H_2NMe)_2n[Ag_2(DMF)_2(Mo_8O_{26})]_n \cdot 2DMF$, and a two-dimensional cross-linked network $([Ag(DMF)]_2[Ag(DMF)_2]_2[Mo_8O_{26}]_n)$. Each compound has been characterized by single-crystal X-ray diffraction, elemental analysis, and FT-IR.

Introduction

Polyoxometalates (POMs), anionic early transition metal-oxide clusters, provide unrivaled structural diversity combined with a wide range of unique physical properties and nuclearities which range from 6 to 368 metal ions in a single molecule. At the extreme, the largest of this family of poly-anions are truly macromolecular, rivaling the size of proteins, and are thought to be formed by a series of self-assembly processes.¹ Formally, POM clusters are assembled from metal-oxide building blocks with the general formula MO_x ($M = Mo, W, V$, and sometimes Nb and $x = 4-7$). The unique physical properties of POM-based materials are a direct result of their versatile structures and their abilities to delocalize electrons, incorporate hetero-anions, electrophiles, and ligands, and encapsulate guest molecules within a metal-oxide-based cage. POM clusters have been shown to exhibit superacidity,² catalytic activity,² photochemical activity,³ ionic conductivity,³ reversible redox behavior,⁴ bistability,³ and cooperative electronic phenomena.⁵ Furthermore, during the past few years, POM chemistry has continued its development, both as a pure chemical science and also with many new dimensions in a multidisciplinary context,⁶ interacting with other disciplines, such as materials science,^{7,8} nanotechnology,⁹ and biology.¹⁰⁻¹³

Traditionally, standard synthetic methods in POM chemistry employ one-pot reactions to create structures of phenomenal diversity and of a wide range of nuclearities. As a result, however, this approach allows only a very limited control over the complicated relationship between synthetic conditions, mechanism of assembly, and molecular structure.^{1,6,14,15} Therefore, the systematic manipulation of each of the many reaction parameters often represents a straightforward, but rather tedious, route to novel POM clusters.¹ The development of a building-block approach that utilizes synthetic equivalents or synthons that can be connected by predefined linkers could provide an elegant solution.¹⁶ This approach would allow scientists to assemble large clusters or networks from smaller known building

blocks and could offer a direct way to systematically control the overall cluster architecture and properties. It would further provide access to the growth of nanoscopic cluster systems of predetermined structure and function via a bottom-up route. Thus, research toward understanding and manipulation of the self-assembly processes that underpin the formation of POM clusters has to be an attractive way to enable the design of multifunctional materials, which take advantage of the unique physical properties associated with such clusters.²⁻¹³

In our recent work, we have been striving toward this goal, and it has been established that the major problem is to produce building blocks which are reactive enough to be reliably utilized in the formation of larger assemblies but, on the other hand, stable enough to be assembled without reorganizing to other unknown fragments. Access to such building blocks has been the major limitation in the stepwise growth of Mo-based POM clusters compared to the more kinetically inert W-based clusters which have shown some degree of control.¹⁷ Such limitations may be circumvented by adopting an approach that kinetically stabilizes the building blocks in solution, thereby effectively preventing their reorganization to other structure types. While developing strategies toward this goal, we recently reported a new family of POMs,¹⁸⁻²¹ which appears to achieve the first part of this objective and allows the isolation of a new structure type by virtue of the cations used to encapsulate this unit, thereby limiting its reorganization to a simpler structure. By using this approach, we have isolated $\{Mo_{16}\}^{18} \equiv [H_2Mo^V_4Mo^VI_{12}O_{52}]^{10-}$, $\{M_{18}\}^{19} \equiv [M_{18}O_{54}(SO_3)_2]^{4-}$ ($M = Mo$ or W), $\{W_{19}\}^{20} \equiv [H_4W_{19}O_{64}]^{6-}$, and $\{W_{36}\}^{21} \equiv [H_{12}W_{36}O_{120}]^{12-}$ by using bulky organic cations such as hexamethylene tetramine and triethanol amine.¹⁸⁻²¹ Thus, the use of bulky organic cations in the formation of Mo-based POMs appears to restrict aggregation to the more highly symmetrical clusters, allowing a fundamentally more diverse set of clusters and cluster-based building blocks to be isolated. These clusters and cluster-based building blocks display unprecedented structural¹⁸ or physical^{19,20} features.

In our previous work, we outlined how counterions can influence the overall architecture of a series of Ag–Mo-POM-

* To whom correspondence should be addressed. E-mail: L.Cronin@chem.gla.ac.uk.

based clusters.^{22,23} As a transition metal, silver(I) is one of the most versatile ions displaying a range of geometries and forming between two and seven coordination bonds, both properties making it a prime candidate to act as a linker.^{24,25} The discovery of the [Ag–Mo₈O₂₆–Ag] synthon in solution has allowed us to clearly identify the location and number of the potential binding sites within this synthon. In this way, the directionality and connectivity at the known binding sites can be predetermined, and to some extent, the overall architecture of the resulting POM can be predicted. The [Ag{Mo₈}Ag] synthon is also an excellent example of how a reactive building block in solution can be manipulated to produce isolated or connected cluster structures.

The first Ag–Mo-based POM with a short Ag–Ag interaction of 2.873 Å was reported by Gouzerh et al. in 1998.²⁵ In this structure, a short Ag–Ag contact is established between two silvers that connect two {Mo₅O₁₃} clusters and results in the formation of a {Ag₂}-bridged discrete dimeric complex. This initial observation of the ability of silver centers to act as linking units in POM-based systems sparked a considerable amount of research and led to the discovery of several molybdenum- and tungsten-based, silver-linked supramolecular rings,²⁶ one-dimensional (1D) chains,^{26–29} two-dimensional (2D) networks^{30,31} as well as monomeric units.^{32,33} Notably, one monomeric cluster, Ag₅PV₂Mo₁₂O₄₀, has been shown to selectively catalyze O₂-mediated sulfoxidation reactions and demonstrates the huge potential of silver–polyoxometalate composites.³³

Herein, we report the successful extension of this encapsulating strategy to the assembly of five novel polymeric architectures based on the coordination of electrophilic silver(I) ions to the well-known β-octamolybdate β-[Mo^{VI}₈O₂₆]^{4–} anion ({Mo₈}): one intermediate chain-like assembly ((Ph₄P)₂[Ag₂(CH₃CN)₂(Mo₈O₂₆)] (1)), three 1D chains ([Ag(C₇H₁₂O₂N)(CH₃CN)]₂[Ag₂(CH₃CN)₂(Mo₈O₂₆)]·2CH₃CN (2), (Ph₄P)₂[Ag₂(DMF)₂(Mo₈O₂₆)]·2DMF (3), and (H₂NMe₂)₂[Ag₂(DMF)₂(Mo₈O₂₆)]·2DMF (4)), where the solvent acts as ligand or spacer or through decomposition of solvent molecules to become counterions, and finally, a 2D DMF solvent pillared array ((Ag(DMF))₂(Ag(DMF))₂Mo₈O₂₆)]_n (5)). Previously, we presented the first examples of the family of Ag–{Mo₈}–based polyoxometalates,²² which range from monomeric synthons ((Ph₄P)₂[Ag₂(DMSO)₄Mo₈O₂₆]] (6) to chains ((n-Bu₄N)_{2n}[Ag₂Mo₈O₂₆]]_n (7) and (n-Bu₄N)_{2n}[Ag₂Mo₈O₂₆(CH₃CN)₂]]_n (8)), grids (((n-Bu₄N)_{2n}[Ag₂Mo₈O₂₆(DMSO)₂]]_n (9)), and 2D networks (((HDMF)_n[Ag₃(Mo₈O₂₆)(DMF)₄]]_n (10)), see Figure 1. Here, we unify our previous study (structures 6–10)²² with our new work (structures 1–5) and make a full contextual analysis. This analysis is extremely powerful because we are able to present an overall picture that brings together the many insights and begins to allow the development of a general route to the assembly of complex silver–polyoxometalate arrays.

Experimental Section

General Considerations. All [Mo₆O₁₉]^{2–} salts were prepared according to the literature and substituted for the relevant cation.²² (Ph₄P)₂[Ag₂(DMSO)₄(Mo₈O₂₆)] was prepared according to the literature.²² All other chemicals and solvents were commercially purchased and used without further purification.

Preparation of (Ph₄P)₂[Ag₂(CH₃CN)₂(Mo₈O₂₆)]·2CH₃CN (1). (Bu₄N)BF₄ (6.7 mg, 0.02 mmol) was added to a solution of (Ph₄P)₂[Ag₂(Mo₈O₂₆)(DMSO)₄]²² (50 mg, 0.02 mmol) in acetonitrile (6 mL). After the solution was stirred for 1 week, a gray precipitate was filtered off the colorless solution from which colorless crystals were obtained when the solution was left open to the air overnight. The crystallization of the remaining solution by the diffusion of diethyl

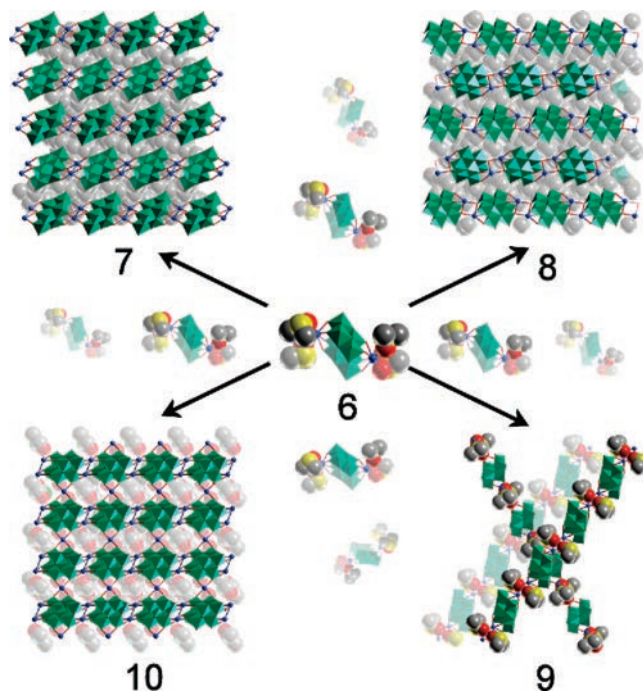


Figure 1. Summary of the structures isolated from the silver–octamolybdate reaction system illustrating the monomer (6), 1D chains (7, 8), grid (9), and 2D network (10). Color scheme: {Mo₈} polyhedra, green; O, red; C, gray; N, light green; and S, yellow.

ether and ethanol over two days resulted in colorless rectangular single crystals. Yield: 22 mg (9.8 μmol, 45% based on Mo). Elemental analysis for C₅₆H₅₂Ag₂Mo₈N₄O₂₆P₂ (%). Calcd: C, 29.99; H, 2.34; N, 2.50. Found: C, 29.95; H, 2.31; N, 2.55. FT-IR (KBr) ν/cm^{–1}: 3448(b), 3059(m), 2927(m), 1584(m), 1482(m), 1438(s), 1316(m), 1189(m), 1109(s), 997(m), 945(s), 904(s).

Preparation of [Ag(C₇H₁₂O₂N)(CH₃CN)]_{2n}[Ag₂(CH₃CN)₂(Mo₈O₂₆)]_n·2CH₃CN (2). A solution of silver(I) nitrate (38 mg, 0.22 mmol) and 2,6-pyridine dimethanol (30 mg, 0.22 mmol) in water (2 mL) was added dropwise to a solution of (n-Bu₄N)₂Mo₆O₁₉ (75 mg, 0.055 mmol) in acetonitrile (5 mL). After the solution was stirred for 4 h, a clear colorless solution was formed, which yielded colorless block crystals by the diffusion of ethanol over three days. Yield: 32 mg (15 μmol, 36% based on Mo). Elemental analysis for C₂₆H₃₆Ag₄Mo₈N₈O₃₀ (%). Calcd: C, 14.59; H, 1.69; N, 5.23. Found: C, 12.82; H, 1.47; N, 3.96 (indicates the loss of two solvent acetonitrile molecules after drying). FT-IR (KBr) ν/cm^{–1}: 3425(s), 2929(w), 1603(m), 1578(m), 1443(w), 1361(w), 1066(m), 936(s), 896(s), 828(s), 794(s), 715(s).

Preparation of (Ph₄P)_{2n}[Ag₂(DMF)₂(Mo₈O₂₆)]_n·2DMF (3). Silver(I) nitrate (33 mg, 0.19 mmol) was dissolved in DMF (2 mL) and added dropwise to a DMF solution (5 mL) of (Ph₄P)₂Mo₆O₁₉ (150 mg, 0.096 mmol) under stirring. The mixture was covered and stirred for 20 h at room temperature. After this time, the solution was still transparent yellow. Colorless needle crystals were successfully grown by the diffusion of diethyl ether or ethanol over three days. Yield: 48 mg (0.02 mmol, 28% based on Mo). Elemental analysis for C₆₀H₆₈Ag₂Mo₈N₄O₃₀P₂ (%). Calcd: C, 30.40; H, 2.89; N, 2.36. Found: C, 29.82; H, 2.58; N, 1.92. FT-IR (KBr) ν/cm^{–1}: 3436(b), 3062(m), 2924(m), 1655(s), 1584(m), 1484(m), 1438(s), 1381(s), 1107(s), 997(s), 947(s), 826(s), 723(s), 527(s).

Preparation of (H₂NMe₂)_{2n}[Ag₂(DMF)₂(Mo₈O₂₆)]_n·2DMF (4). Silver(I) nitrate (34 mg, 0.20 mmol) was dissolved in DMF (2 mL) and added dropwise to a DMF solution (5 mL) of ((n-C₆H₁₃)₄N)₂Mo₆O₁₉ (159 mg, 0.10 mmol) under stirring. The mixture was covered and stirred for 20 h at room temperature. After this time, the solution was still transparent yellow. Colorless block crystals were successfully grown by the diffusion of diethyl ether over 20 days. Yield: 17 mg (0.010 mmol, 13% based on Mo). Elemental analysis for C₁₆H₄₄Ag₂Mo₈N₆O₃₀ (%). Calcd: C, 10.78; H, 2.48; N, 4.71. Found: C, 10.83; H, 2.43; N, 4.56. FT-IR (KBr) ν/cm^{–1}: 3441 (b), 2926 (m),

Table 1

	1	2	3	4	5
formula	C ₅₆ H ₅₂ Ag ₂ Mo ₈ N ₄ O ₂₆ P ₂	C ₂₆ H ₃₆ Ag ₄ Mo ₈ N ₈ O ₃₀	C ₆₀ H ₆₈ Ag ₂ Mo ₈ N ₄ O ₃₀ P ₂	C ₁₆ H ₄₄ Ag ₂ Mo ₈ N ₆ O ₃₀	C ₁₈ H ₄₂ Ag ₄ Mo ₈ N ₆ O ₃₂
<i>M_r</i> [g mol ⁻¹]	2242.22	2139.63	2370.38	1783.83	2053.58
crystal system	triclinic	triclinic	monoclinic	triclinic	triclinic
space group	<i>P</i> $\bar{1}$	<i>P</i> $\bar{1}$	<i>P</i> 2 ₁ / <i>n</i>	<i>P</i> $\bar{1}$	<i>P</i> $\bar{1}$
<i>a</i> [Å]	9.7210(3)	9.6535(3)	17.1720(5)	10.0246(7)	10.1101(2)
<i>b</i> [Å]	11.7984(5)	10.8471(3)	9.2312(3)	10.5735(7)	11.4232(3)
<i>c</i> [Å]	16.0976(7)	12.1151(3)	24.0351(3)	11.8724(6)	11.5474(3)
α [°]	85.561(2)	80.068(2)	90	85.711(4)	63.312(1)
β [°]	75.929(2)	82.5150(10)	100.400(2)	65.494(4)	76.600(2)
γ [°]	68.078(2)	85.153(2)	90	69.821(3)	88.951(1)
ρ_{calc} [g cm ⁻³]	2.241	2.874	2.101	2.765	2.956
<i>V</i> [Å ³]	1661.20(11)	1236.44(6)	3747.41(18)	1071.33(12)	1153.43(5)
<i>Z</i>	1	1	2	1	1
$\mu(\text{Mo K}\alpha)$ [mm ⁻¹]	2.163	3.598	1.928	3.251	3.852
<i>T</i> [K]	150(2)	150(2)	150(2)	150(2)	150(2)
no. rflns (measd)	23586	17497	22707	15097	15599
no. rflns (unique)	6500	4844	6845	4195	4455
no. params	444	349	492	287	314
<i>R</i> 1 (<i>I</i> > 2 σ (<i>I</i>))	0.0450	0.0229	0.0423	0.0425	0.0255
<i>wR</i> 2 (all data)	0.0750	0.0538	0.0865	0.0828	0.0525

1654 (s), 1386 (s), 1259 (s), 1104 (s), 946 (s), 915 (s), 846 (m), 709 (s), 664 (s), 561 (s), 525 (s), 415 (s).

Preparation of [(Ag(DMF))₂(Ag(DMF))₂Mo₈O₂₆]_{*n*} (5). Silver(I) nitrate (34 mg, 0.20 mmol) suspended in DMF (2 mL) and was added dropwise to a solution of ((*n*-C₇H₁₅)₄N)₂Mo₈O₁₉ (148 mg, 0.09 mmol) in DMF (5 mL). The solution was stirred overnight. After this time, a yellow solution had formed with some brown precipitate. The filtration of this solution yielded a clear yellow solution from which colorless block crystals were obtained through the diffusion of diethyl ether for five days and were suitable for single-crystal X-ray diffraction. Yield: 11 mg (0.01 mmol, 8% based on Mo). Elemental analysis for C₁₈H₄₂Ag₄Mo₈N₆O₃₂ (%). Calcd: C, 10.53; H, 2.06; N, 4.09. Found: C, 8.72; H, 1.83; N, 3.53 (indicates the loss of one DMF molecule). FT-IR (KBr) ν/cm^{-1} : 3433(b), 2924(w), 2873(s), 1656 (vs), 1414 (w), 1384 (w), 1252 (w), 1107 (m), 947 (vs), 905 (vs), 842 (m), 714 (s).

Single-Crystal Structure Determination. Suitable single crystals of **1–5** were grown and mounted onto the end of a thin glass fiber by using Fomblin oil. The X-ray diffraction intensity data were measured at 150 K on a Nonius Kappa-CCD diffractometer [$\lambda(\text{Mo K}\alpha) = 0.71073$ Å], graphite monochromator. The structure solution and refinement for **1–5** was carried out with the SHELXS-97³⁴ and SHELXL-97³⁵ programs via WinGX.³⁶ The corrections for the incident and diffracted beam absorption effects were applied using empirical³⁷ or numerical methods.³⁸ Compounds **1**, **2**, **4**, and **5** crystallized in the space group *P* $\bar{1}$ and compound **3** in *P*2₁/*n*, as determined by the systematic absences in the intensity data, the intensity statistics, and the successful solution and refinement of the structures. All the structures were solved by a combination of direct methods and difference Fourier syntheses and refined against *F*² by the full-matrix least-squares technique. The crystal data, data collection parameters, and refinement statistics for **1–5** are listed in Table 1. These data can also be obtained free of charge via www.ccdc.cam.ac.uk/conts/retrieving.html or from the Cambridge Crystallographic Data Center (12 Union Road, Cambridge CB2 1EZ. Fax: (+44) 1223-336-033 or deposit@ccdc.cam.ac.uk).

Results and Discussion

General Considerations for the Interactions of {Mo₈} with Ag(I). Recently, it has been discovered within our group that the well-known β -octamolybdate (β -[Mo₈O₂₆]⁴⁻ = {Mo₈}) cluster can be used as an inorganic scaffold with the ability to bind different transition metals such as silver(I).²² Our results demonstrate that the favored binding sites for Ag(I) centers are the weakly nucleophilic terminal oxygen atoms, which are sterically favored over the bridging μ_2 -oxygens. It has furthermore been shown that, depending on the exact reaction conditions, the silver centers can occupy different coordination sites and therefore offer excellent possibilities for linking the {Mo₈} groups into a whole range of 1D and 2D supramolecular

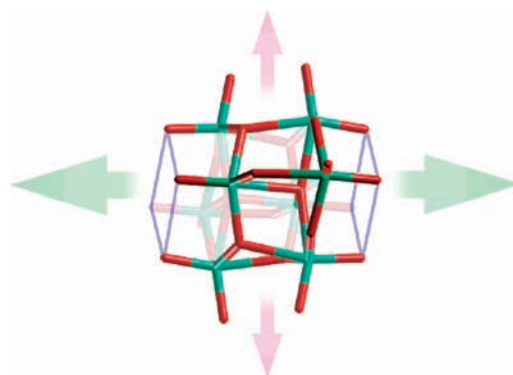


Figure 2. Representation of the β -[Mo₈O₂₆] building block illustrating the two preferred binding sites. The two tetrahedral {O₄} binding sites are highlighted with blue squares. The arrows indicate the direction of the structural growth along the primary (green arrows) and secondary (pink arrows) binding sites. Color scheme: Mo, green and O, red.

assemblies. The preferred primary binding sites of the cluster are two distinct square-planar arrangements of four terminal oxygen atoms ({O₄}) with O–O distances between 3.0 and 3.2 Å, see Figure 1. The two {O₄} faces are arranged in a coparallel fashion and therefore allow the transition-metal-mediated assembly of multiple {Mo₈} groups into linear supramolecular structures. The secondary binding sites are two sets of two terminal oxygen atoms with O–O distances of ca. 3.0 Å, which act as bidentate chelating ligands and are arranged perpendicularly to the primary {O₄} moieties, see Figure 2. This spatial orientation allows the extension of the structural growth from unidimensional chains into 2D gridlike nets. The framework extension into three-dimensional (3D) structures can theoretically be achieved by employing the two remaining terminal oxygen atoms as they are arranged orthogonally to the first two coordination sites.

Structural Analysis of (Ph₄P)₂[Ag₂(CH₃CN)₂(Mo₈O₂₆)]·2CH₃CN (1). The study of a range of structurally related compounds provided a unique insight into the self-assembly processes that occur in the silver–octamolybdate reaction system. In an attempt to control this self-assembly process, organic counterions were utilized to influence the architecture of the polyoxometalates assemblies. This strategy was successfully extended by employing an existing monomeric [Ag{Mo₈}Ag] cluster and subsequently growing this isolated

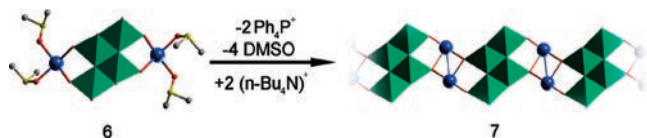


Figure 3. Illustration of the molecular growth of the isolated unit **7** into the 1D polymer **6** via a cation-exchange route. Color scheme: {Mo₈}, green; Ag, light blue spheres; C, gray; and S, yellow (hydrogen atoms and cations removed for clarity).

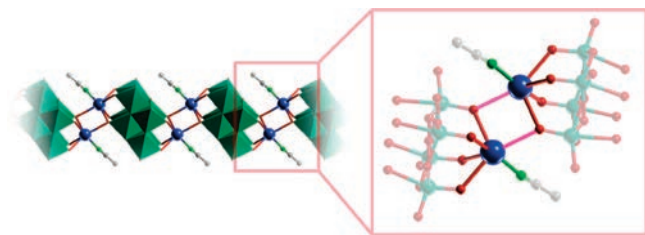


Figure 4. Left: Illustration of the supramolecular assembly in compound **1**. Right: Detailed illustration of the connectivity of the silver ions, highlighting the two long-range (ca. 2.8 Å) Ag–O contacts (pink) which connect the clusters. Color scheme: {Mo₈} and Mo, green; Ag, light blue spheres; C, gray; and N, light green (cations, solvent molecules, and hydrogen atoms removed for clarity).

structure (**6**) into a 1D polymer, $(n\text{-Bu}_4\text{N})_{2n}[\text{Ag}_2(\text{Mo}_8\text{O}_{26})]_n$ (**7**), which contains {Mo₈} units linked in one dimension by {Ag₂} dimers.²² One major driving force of this self-assembly was the use of bulky but flexible tetra-*n*-butyl ammonium ($n\text{-Bu}_4\text{N}^+$) cations which have the ability to isolate the inorganic building blocks and form an organic scaffold that causes the restricted aggregation and eventually the growth of the [Ag{Mo₈}Ag] building blocks into a 1D structure, see Figure 3.

Similar synthetic conditions were therefore employed in order to allow the self-aggregation of the isolated unit $(\text{Ph}_4\text{P})_2[\text{Ag}_2(\text{DMSO})_4(\text{Mo}_8\text{O}_{26})]$ (**6**). Compound **6** was reacted stoichiometrically with $(n\text{-Bu}_4\text{N})\text{BF}_4$ in acetonitrile to replace the rigid bulky tetra-phenyl phosphonium groups with the flexible aliphatic ammonium counterion $n\text{-Bu}_4\text{N}^+$. The structural analysis of the single-crystalline reaction product, however, showed that a novel unit, $(\text{Ph}_4\text{P})_2[\text{Ag}_2(\text{CH}_3\text{CN})_2(\text{Mo}_8\text{O}_{26})]$ (**1**), had been synthesized, in which formally the four DMSO ligands present in the precursor **7** were replaced by two acetonitrile ligands. This ligand exchange has a dramatic effect on the overall structure of the supramolecular assembly, as it creates a vacancy in the coordination sphere of the Ag(I) center, allowing the silver to establish a long-range (ca. 2.8 Å) Ag–O contact to an adjacent {Mo₈} cluster, and as a result, this bond formation leads to the linking of the particular clusters into a supramolecular array, see the left part of Figure 4. The detailed structural analysis of the silver coordination environment shows that each silver(I) ion binds to one {Mo₈} cluster by coordinating to a tetradentate {O₄} square face through four Ag–O bonds with bond lengths of 2.3–2.7 Å. The Ag coordination sphere is further filled by a CH₃CN ligand, which binds to the silver through its nitrogen atom in an end-on fashion, see the right part of Figure 4.

In contrast to compound **7**, no {Ag₂} dimer formation can be observed in **1** because the Ag–Ag distance of 3.647 Å is substantially longer than the sum of the van der Waals radii (3.44 Å). The chain is therefore solely held together by the long-range Ag–O contacts described above, and hence, the assembly shows only weak attractive interactions between the

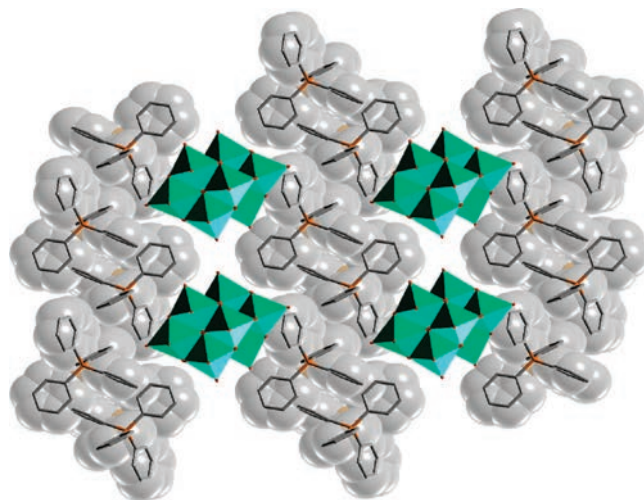


Figure 5. View of **1** along the crystallographic *a*-axis, illustrating how the chains are embedded in the layers of organic counterions. Color scheme: {Mo₈}, green polyhedra; C, gray; and P, orange (Ag ions, solvent molecules, and hydrogen atoms removed for clarity).

[Ag{Mo₈}Ag] building blocks and has to be considered an intermediate rather than a true polymeric structure.

In the lattice, the polymeric chains are arranged in a collinear fashion and are separated by the organic counterion tetra-phenyl phosphonium (Ph_4P^+). The presence of these bulky cations is vital for the isolation of this 1D intermediate, because their rigid structure keeps the chains separated and thereby prohibits any further cross-linking into networks of higher dimensionality, see Figure 5. Furthermore, the organic counterions interact with the cluster via C–H···O hydrogen bonds.

Compound **1** represents a rare example of an intermediate between isolated monomers, such as **7**, where each silver ion is exclusively bound to one {Mo₈} unit, and {Ag₂}-bridged coordination polymers, such as **6**, where the silver centers link two clusters by argentophilic Ag–Ag interactions as well as by Ag–O coordination bonds. The isolation of **1**, where the silver(I) ions act as linkers between the particular {Mo₈} units but in which no argentophilic Ag–Ag bond formation can be observed, might provide a unique insight into the assembly mechanism which leads to the formation of {Ag₂} dimer assemblies.

Structural Analysis of $[\text{Ag}(\text{C}_7\text{H}_{12}\text{O}_2\text{N})(\text{CH}_3\text{CN})]_{2n}\text{-}[\text{Ag}_2(\text{CH}_3\text{CN})_2(\text{Mo}_8\text{O}_{26})]_n \cdot 2\text{CH}_3\text{CN}$ (2**).** The reaction of $(n\text{-Bu}_4\text{N})_4[\text{Mo}_6\text{O}_{19}]$ with silver(I) nitrate was investigated in the presence of 2,6-pyridine dimethanol in order to replace the bulky organic ammonium cation and to establish the structural influence of a planar aromatic coordinating compound. The single-crystal XRD analysis of the product showed that the $n\text{-Bu}_4\text{N}^+$ cation had been successfully replaced, and a complex supramolecular assembly of the formula $[\text{Ag}(\text{C}_7\text{H}_{12}\text{O}_2\text{N})(\text{CH}_3\text{CN})]_{2n}[\text{Ag}_2(\text{CH}_3\text{CN})_2(\text{Mo}_8\text{O}_{26})]_n \cdot 2\text{CH}_3\text{CN}$ (**2**) had been obtained. The detailed structural analysis revealed that the [Ag{Mo₈}Ag] synthons in **2** are arranged in a unidimensional assembly, in which {Ag₂} dimers link the {Mo₈} clusters into linear polymeric chains (see the left part of Figure 6). The building units of these chains are structurally closely related to the intermediate species in **1** but show distinctive differences in the way the {Mo₈} clusters are linked. Each silver occupies one square {O₄} face of a {Mo₈} cluster and links to the adjacent cluster by forming two long-range coordinative Ag–O bonds (Ag–O distances of 2.8–2.9 Å), which in turn align the two adjacent Ag(I) centers in a way that allows the formation of a

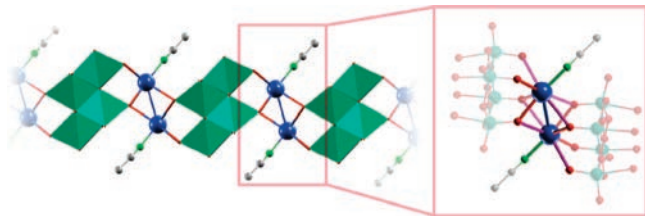


Figure 6. Left: Illustration of the polymeric chain in **2** along the crystallographic *a*-axis. Right: Detailed illustration of the connectivity of the $\{Ag_2\}$ dimeric linker in **2**. Note the long-range Ag–O bonds marked in pink. Color scheme: Mo and $\{Mo_8\}$ -polyhedra, green; Ag, light blue spheres; O, red; N, dark blue; and C, gray (counterions, solvent molecules, and hydrogen atoms removed for clarity).

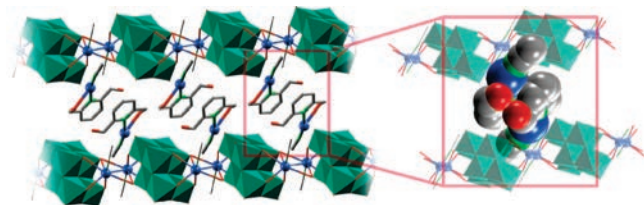


Figure 7. Left: Representation of the crystal lattice of **2**, illustrating the layered arrangement of the chains and counterions. Right: Space-filled representation of the complex cation $[Ag(C_7H_{12}O_2N)(CH_3CN)]^+$, highlighting its separating effect. Color scheme: $\{Mo_8\}$ polyhedra, green; Ag, blue spheres; O, red; N, light green; and C, gray (solvent molecules and hydrogen atoms removed for clarity).

dimeric $\{Ag_2\}$ moiety with the short Ag–Ag distances of 3.181 Å. The primary Ag coordination shell is completed by one acetonitrile molecule which points away from the oxygen environment, thereby minimizing the ligand repulsion, see the right part of Figure 6.

In the lattice, the polymeric chains are separated by the complex cations formed by a Ag(I) center which coordinates to the planar aromatic ligand 2,6-pyridine dimethanol (see Figure 6) via one Ag–N and one Ag–O coordination bond. These complex counterions evidently have the ability to restrict the further aggregation of the 1D chain, thus preventing the $[Ag\{Mo_8\}Ag]$ synthon from forming 2D networks. The structural analysis of the cationic silver complex shows that the Ag binds to the organic ligand via one Ag–N and one Ag–O bond with one additional acetonitrile, completing the trigonal Ag coordination sphere. In the lattice, adjacent cations are π - π -stacked in an offset fashion in order to allow the maximum orbital overlap and to increase the overall framework stability (see Figure 7). Interestingly, the second CH_2OH arm of the 2,6-pyridine dimethanol is not engaged in coordinative interactions with the silver ion, but preferably forms hydrogen bonds to a terminal Mo=O group, which reinforces the framework.

Structural Analysis of $(Ph_4P)_2n[Ag_2(DMF)_2(Mo_8O_{26})]_n \cdot 2DMF$ (3**).** The reaction of $(Ph_4P)_2Mo_6O_{19}$ with silver(I) nitrate was studied in the presence of the highly coordinating solvent DMF in order to establish the influence of the solvent effects on the formation of extended assemblies. The single-crystal XRD analysis of the reaction product indicated the presence of a complex Ag– $\{Mo_8\}$ -based framework with the composition $(Ph_4P)_2n[Ag_2(DMF)_2(Mo_8O_{26})]_n \cdot 2DMF$ (**3**). The detailed structural characterization showed that the main component in **3** is a 1D polymeric chain, resembling the chain in **2**, in which the $\{Mo_8\}$ clusters are connected by $\{Ag_2\}$ linkers, which coordinate to the tetradentate faces of adjacent octamolybdates, see the left part of Figure 8.

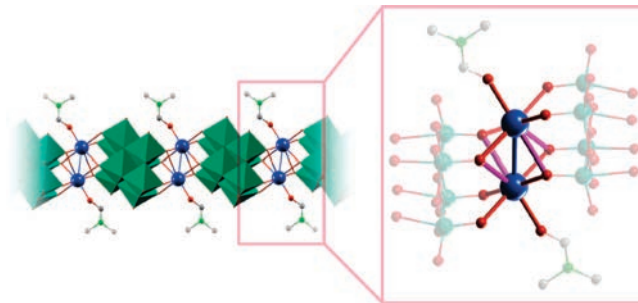


Figure 8. Left: Illustration of the polymeric chain in **3** along the crystallographic *a*-axis. Right: Detailed illustration of the connectivity of the $\{Ag_2\}$ dimer. Note the long-range Ag–O bonds (>2.8 Å) in pink. Color scheme: $\{Mo_8\}$ polyhedra and Mo, green; Ag, blue spheres; O, red; N, light green; and C, gray (counterions, hydrogen atoms, and solvent molecules removed for clarity).

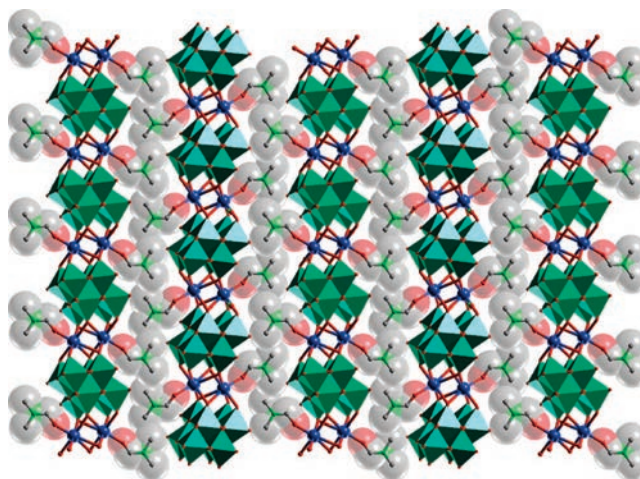


Figure 9. Illustration of compound **3** along the crystallographic *a*-axis, highlighting the collinear arrangement of the polymer chains directed by the DMF spacers. Color scheme: $\{Mo_8\}$ polyhedra, green; Ag, blue spheres; O, red; N, light green; and C, gray (counterions, solvent molecules, and hydrogen atoms removed for clarity).

In contrast to **2**, however, the primary coordination environment around the Ag centers in **3** is a square-planar arrangement of four terminal oxygen atoms with Ag–O bond lengths of 2.4–2.5 Å, which results in a planar linking motif, see the right part of Figure 6. Furthermore, the silver ions form long-range coordinative bonds to the two remaining oxygens of one $\{O_4\}$ face (Ag–O bond length ca. 2.85 Å), which reinforce the structural stability of the supramolecular chain and allow the formation of $\{Ag_2\}$ dimers with the short Ag–Ag contacts of 3.1299 Å, see the right part of Figure 7. The Ag coordination sphere is filled by a DMF molecule which coordinates to the silver via its oxygen atom and in effect acts as an organic spacer which keeps the collinear chains separated, see the left part of Figure 8.

Interestingly, compound **3** shows two different features that allow the growth of the starting material into a 1D chain but exclude the formation of extended 2D or 3D networks. Primarily, the bulky and rigid Ph_4P^+ cations act as large spacers which prevent the formation of further cross-links between the particular chains and force the chains into a collinear layered arrangement. However, the silver-bound DMF ligands act not purely as capping ligands but as spacers and thereby exclude any intralayer cross-linking interactions between adjacent chains within one layer, see Figure 9. Compound **3** also represents an

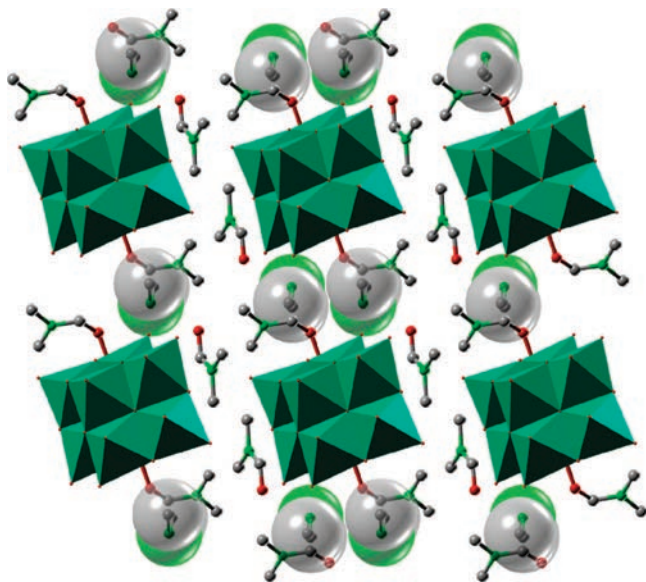


Figure 10. Representation of the crystal packing of **4** along the crystallographic *a*-axis, emphasizing the separating effect of the organic counterions. Color scheme: {Mo₈} polyhedra, green; Ag, light blue spheres; C, gray; N, light green; and O, red (hydrogen atoms removed for clarity).

intriguing contrast to the monomeric structure **7**, (Ph₄P)₂[Ag₂(DMSO)₄Mo₈O₂₆], which has been discussed earlier. In **7**, the use of the bulky Ph₄P⁺ cations and of DMSO as a coordinating solvent allows the isolation of a monomeric [Ag₂(DMSO)₄Mo₈O₂₆] unit, whereas, in compound **3**, DMF does not have the ability to stop the chain growth, and therefore, a polymeric product is formed.

Structural Analysis of (H₂NMe₂)_{2n}[Ag₂(DMF)₂(Mo₈O₂₆)_n·2DMF (4**).** In this set of experiments, the rigid bulky Ph₄P⁺ cation employed in **3** was replaced by the much more flexible (*n*-C₆H₁₃)₄N⁺ cation to investigate its effect on the reaction system and to confirm our hypothesis that this large cation is indeed too bulky to be included in larger silver-POM assemblies. ((*n*-C₆H₁₃)₄N)₂Mo₆O₁₉ was reacted with silver nitrate in the presence of DMF, and the single-crystal XRD studies of the crystalline product revealed the formation of (H₂NMe₂)_{2n}[Ag₂(DMF)₂(Mo₈O₂₆)_n·2DMF (**4**). The main component of this assembly is again a 1D chain, which shows distinct structural similarities to the polymeric chain in compound **3**. In structure **4**, the {Mo₈} synthons are interconnected by {Ag₂} linkers, which form short coordinative Ag–O bonds (bond length 2.4–2.5 Å), to four terminal oxygens in a square-planar arrangement and thereby create a link between two adjacent clusters. In a fashion similar to **3**, the silver ions complete their oxygen coordination environment by forming two long-range Ag–O contacts (Ag–O distance ca. 2.8 Å) to the two remaining terminal oxygens of one {O₄} square face. The coordination sphere of each Ag(I) center is completed by one DMF ligand, which is arranged perpendicularly to the direction of the chain propagation and therefore inhibits the cross-linking of the particular 1D chains into networks. As already discussed for compound **3**, this spatial arrangement allows a high orbital overlap between the two d¹⁰ Ag centers and results in the short Ag–Ag distances of 3.0201 Å. Interestingly, in contrast to the crystal lattice in **3**, the chains in this compound are separated by protonated dimethyl ammonium cations, which have been produced by an in situ decomposition of the solvent DMF, resulting in a closely packed, layered

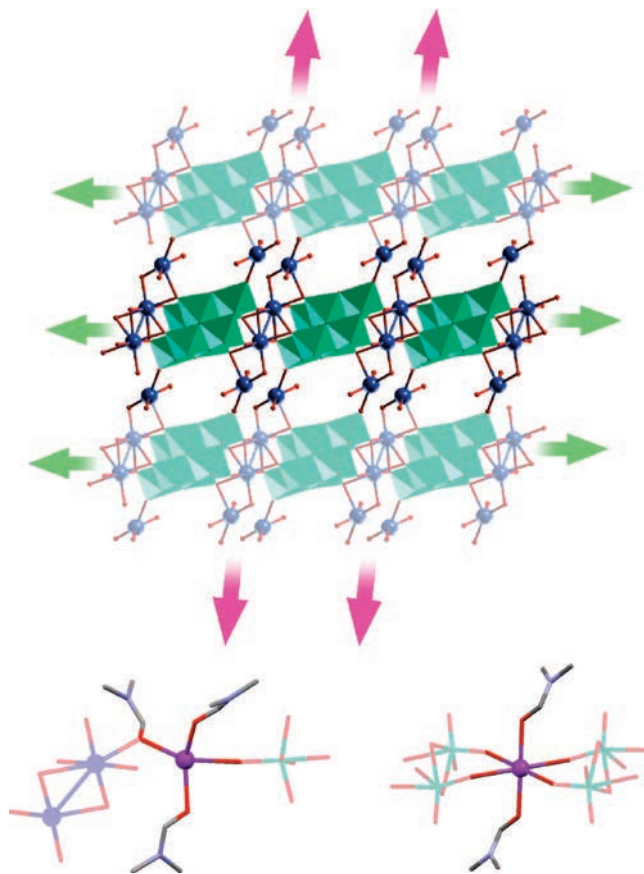


Figure 11. Top: View of the network arrangement in **5** along the crystallographic *c*-axis, illustrating the supramolecular arrangement into a 2D grid. Green and pink arrows indicate the directions of the primary and secondary linking, respectively. Bottom: Detailed illustration of the different linking modes of the isolated silver(I) linking unit (purple sphere) in **5** (left) and in **10** (right). Color scheme: Mo, green; {Ag₂} dimer, light blue spheres; C, gray; and N, blue (hydrogen atoms removed for clarity).

arrangement of polymeric chains and of dimethyl ammonium cations which form hydrogen bonds to the {Mo₈} units and thus reinforce the structure, see Figure 10. Further structural stability is provided by DMF solvent molecules which increase the network of hydrogen bonds.

The virtually planar dimeric [{O₂AgO₂}]₂ bridging motifs in structures **3** and **4** seem to represent a common binding motif and have also been observed in structure **6** and in a structure reported by Gouzerh et al.²⁵ However, in contrast to the latter ones, the [{O₂AgO₂}]₂ motifs in **3** and **4** feature longer Ag–Ag distances, which is most likely a consequence of the presence of terminal DMF ligands, which decrease the orbital overlap efficiency between the two d¹⁰ silver ions.

Structural Analysis of [(Ag(DMF))₂(Ag(DMF))₂Mo₈O₂₆]_n (5**).** The syntheses and structural comparison of compounds **3** and **4** clearly demonstrated the effects that are introduced by the presence of different types of cations. To complete this comprehensive study involving the interaction of the counterion with the solvent DMF, the experimental strategy was extended to using even larger aliphatic amines. ((*n*-C₇H₁₅)₄N)₂Mo₆O₁₉ was reacted with silver(I) nitrate in the presence of DMF and gave a crystalline reaction product which was isolated and characterized by single-crystal XRD analysis. The structural analysis showed that a 2D network of the formula [(Ag(DMF))₂(Ag(DMF))₂Mo₈O₂₆]_n (**5**) had been obtained. The

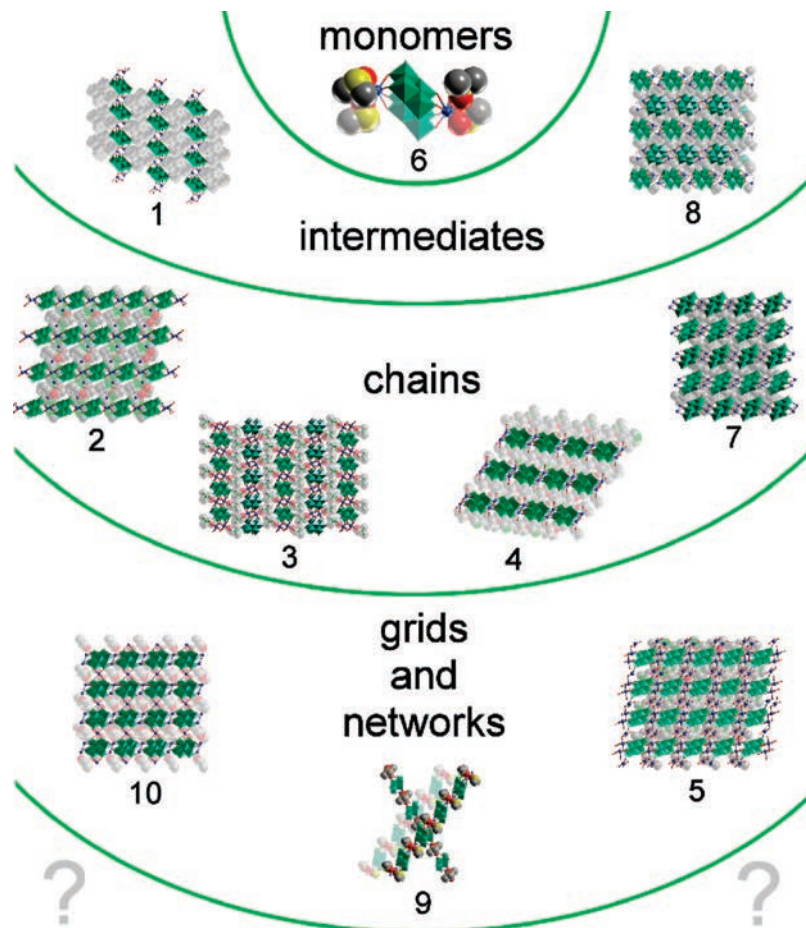


Figure 12. Comprehensive summary of the structures isolated from the silver–octamolybdate reaction system.

primary supramolecular component of this network is a 1D assembly, in which $\{Ag_2\}$ dimers link $\{Mo_8\}$ clusters to form infinite chains along the crystallographic a -axis. This chain resembles the two chain structures reported earlier (compounds **3** and **4**); again, each silver center connects two $\{Mo_8\}$ clusters by coordinating two terminal oxygens of each cluster, resulting in a square-planar geometric arrangement around each central Ag with Ag–O bond lengths of 2.4–2.6 Å. Further structural stability is provided by the formation of two long-range Ag–O bonds (2.7–2.9 Å), and the coordination sphere of the silver ion is completed by one DMF molecule which is coordinated via its oxygen atom. The resulting Ag–Ag dimer bond length of 3.0549(5) Å is comparable to lengths in the structures discussed earlier. In contrast to the previous structures, however, the chains in **5** do not form isolated 1D polymers but are linked by a second type of silver bridges along the crystallographic b -axis to form a truly 2D coordination network, see the top panel of Figure 11. This represents a prime example of the versatility of Ag(I) centers to act as bridging ligands, not only by their ability to self-aggregate into $\{Ag_2\}$ dimers but also by the ability of an isolated Ag(I) center to link two chains. In this case, this is accomplished by the coordination of the silver to a terminal oxygen ligand of one $\{Mo_8\}$ cluster and by engaging the DMF ligand on the $\{Ag_2\}$ dimer of an adjacent chain as a bridging ligand (see the bottom left part of Figure 11). The coordination sphere of this silver bridge is filled by two additional DMF ligands which again bind to the Ag(I) via their oxygen atoms, resulting in a highly distorted square-planar coordination environment. This distinct spatial arrangement contrasts with the cross-linking mode featured in compound **10**,²² where an

isolated silver(I) unit bridges between two collinear chains by exclusively coordinating to terminal Mo=O bonds, see the bottom right part of Figure 11. Again, these results demonstrate the versatility of the Ag(I)– $\{Mo_8\}$ reaction system, where self-assembly allows the reversible formation and eventually the isolation of a multitude of novel silver-linked polyoxometalate assemblies.

Conclusions

This report comprehensively describes synthetic strategies that allow the formation of 1D and 2D structural assemblies obtained by self-assembly processes involving the linking of monomeric $\{Mo_8\}$ groups into chains and networks by virtue of the flexible silver(I) cation, which can adopt several different coordination modes. Figure 12 summarizes these structures. The isolation of **1**, an intermediate between isolated monomeric synthons and polymeric chains, not only allows the detailed study of the silver–molybdate coordination modes but is crucial in understanding the processes which allow the formation of larger silver–polyoxometalate assemblies. Structures **2**, **3**, and **4** represent a logical progression from compound **1**, and they all feature polymeric chains made up of $\{Mo_8\}$ clusters which are linked by $\{Ag_2\}$ dimers. This linking motif is uncommon in polyoxometalate chemistry and represents a rare example of d^{10} closed shell bridging units which are held together by argentophilic interactions. Finally, compound **5** provides further insight into the assembly of silver-linked polyoxometalates and shows how the silver cations can bridge clusters to form extended arrays, by adopting two different connecting modes.

Future work will extend these linking principles and study the formation of functional materials by applying the rules that have been established in this study to other Mo- and W-based polyoxometalate systems, as well as studying the assembly processes in both solution and solid state.

Acknowledgment. The authors would like to thank the University of Glasgow, the EPSRC, the Royal Society, and the Leverhulme Trust for funding.

Supporting Information Available: Structures as CIF files. This information is available free of charge via the Internet at <http://pubs.acs.org>.

References

- (1) (a) Long, D.-L.; Burkholder, E.; Cronin, L. *Chem. Soc. Rev.* **2007**, *36*, 105. (b) Cronin, L. *Comprehensive Coordination Chemistry Reviews 2. Polyoxometalate Clusters*; Elsevier: Amsterdam, 2004; Vol. 7, pp 1–57. (c) Müller, A.; Kögerler, P.; Dress, A. W. M. *Coord. Chem. Rev.* **2001**, *222*, 193. (d) Müller, A.; Peters, F.; Pope, M. T.; Gatteschi, D. *Chem. Rev.* **1998**, *98*, 239.
- (2) (a) Neumann, R.; Dahan, M. *Nature* **1997**, *388*, 353. (b) Mizuno, N.; Misono, M. *Chem. Rev.* **1998**, *98*, 199.
- (3) (a) Katsoulis, D. E. *Chem. Rev.* **1998**, *98*, 359. (b) Yamase, T. *Chem. Rev.* **1998**, *98*, 307.
- (4) (a) Rütger, T.; Hultgren, V. M.; Timko, B. P.; Bond, A. M.; Jackson, W. R.; Wedd, A. G. *J. Am. Chem. Soc.* **2003**, *125*, 10133. (b) Fay, N.; Bond, A. M.; Baffert, C.; Boas, J. F.; Pilbrow, J. R.; Long, D.-L.; Cronin, L. *Inorg. Chem.* **2007**, *46*, 3502. (c) Baffert, C.; Boas, J. F.; Bond, A. M.; Kögerler, P.; Long, D. L.; Pilbrow, J. R.; Cronin, L. *Chem. Eur. J.* **2006**, *12*, 8472.
- (5) Yamase, T.; Fukaya, K.; Nojiri, H.; Ohshima, Y. *Inorg. Chem.* **2006**, *45*, 7698.
- (6) Pope, M. T.; Müller, A. *Angew. Chem., Int. Ed.* **1991**, *30*, 34.
- (7) (a) Casan-Pastor, N.; Gomez-Romero, P. *Front. Biosci.* **2004**, *9*, 1759. (b) Song, Y.-F.; Abbas, H.; Ritchie, C.; McMillan, N.; Long, D.-L.; Gadegaard, N.; Cronin, L. *J. Mater. Chem.* **2007**, *17*, 1903. (c) Song, Y. F.; Long, D.-L.; Cronin, L. *Angew. Chem., Int. Ed.* **2007**, *46*, 3900.
- (8) Khan, M. I. *J. Solid State Chem.* **2000**, *152*, 105.
- (9) Long, D.-L.; Cronin, L. *Chem.-Eur. J.* **2006**, *12*, 3698.
- (10) Ma, H. Y.; Peng, J.; Han, Z. G.; Yu, X.; Dong, B. X. *J. Solid State Chem.* **2005**, *178*, 3735.
- (11) Yamase, T. *J. Mater. Chem.* **2005**, *15*, 4773.
- (12) Hasenknopf, B. *Front. Biosci.* **2005**, *10*, 275.
- (13) Nomiyama, K.; Torii, H.; Hasegawa, T.; Nemoto, Y.; Nomura, K.; Hashino, K.; Uchida, M.; Kato, Y.; Shimizu, K.; Oda, M. *J. Inorg. Biochem.* **2001**, *86*, 657.
- (14) Nyman, M.; Bonhomme, F.; Alam, T. M.; Rodriguez, M. A.; Cherry, B. R.; Krumhansl, J. L.; Nenoff, T. M.; Sattler, A. M. *Science* **2002**, *297*, 996.
- (15) Müller, A.; Beckmann, E.; Bögge, H.; Schmidtman, M.; Dress, A. *Angew. Chem., Int. Ed.* **2002**, *41*, 1162.
- (16) Müller, A.; Kögerler, P.; Kuhlmann, C. *Chem. Commun.* **1999**, 1347.
- (17) Wei, Y.; Xu, B.; Barnes, C. L.; Peng, Z. *J. Am. Chem. Soc.* **2001**, *123*, 4083.
- (18) (a) Long, D.-L.; Kögerler, P.; Farrugia, L. J.; Cronin, L. *J. Chem. Soc., Dalton Trans.* **2005**, 1372. (b) Long, D.-L.; Kögerler, P.; Farrugia, L. J.; Cronin, L. *Angew. Chem., Int. Ed.* **2003**, *42*, 4180.
- (19) (a) Long, D.-L.; Kögerler, P.; Cronin, L. *Angew. Chem., Int. Ed.* **2004**, *43*, 1817. (b) Long, D.-L.; Abbas, H.; Kögerler, P.; Cronin, L. *Angew. Chem., Int. Ed.* **2005**, *44*, 3415.
- (20) Long, D.-L.; Kögerler, P.; Parenty, A. D. C.; Fielden, J.; Cronin, L. *Angew. Chem., Int. Ed.* **2006**, *45*, 4798.
- (21) (a) Long, D.-L.; Brücher, O.; Streb, C.; Cronin, L. *J. Chem. Soc., Dalton Trans.* **2006**, 2852. (b) Long, D.-L.; Abbas, H.; Kögerler, P.; Cronin, L. *J. Am. Chem. Soc.* **2004**, *126*, 13880.
- (22) Abbas, H.; Pickering, A. L.; Long, D.-L.; Kögerler, P.; Cronin, L. *Chem. Eur. J.* **2005**, *11*, 1071.
- (23) Chen, S.-M.; Lu, C.-Z.; Yu, Y.-Q.; Zhang, Q.-Z.; He, X. *Inorg. Chem. Commun.* **2004**, *7*, 1041.
- (24) Pickering, A. L.; Long, D.-L.; Cronin, L. *Inorg. Chem.* **2004**, *43*, 4953.
- (25) Villanneau, R.; Proust, A.; Robert, F.; Gouzerh, P. *Chem. Commun.* **1998**, 1491.
- (26) Ren, Y.-P.; Kong, X.-J.; Long, L.-S.; Huang, R.-B.; Zheng, L.-S. *Cryst. Growth Des.* **2006**, *6*, 57229.
- (27) An, H.; Li, Y.; Wang, E.; Xiao, D.; Sun, C.; Xu, L. *Inorg. Chem.* **2005**, *44*, 6062.
- (28) Shi, Z.; Gu, X.; Peng, J.; Xin, Z. *Eur. J. Inorg. Chem.* **2005**, 3811.
- (29) Chen, J.-X.; Lan, T. Y.; Huang, Y.-B.; Wei, C.-X.; Li, Z.-S.; Zhang, Z.-C. *J. Solid State Chem.* **2006**, *179*, 1904.
- (30) Burkholder, E.; Zubieta, J. *Solid State Sci.* **2004**, *6*, 1421.
- (31) Han, Z.; Zhao, Y.; Peng, J.; Ma, H.; Liu, Q.; Wang, E.; Hu, N.; Jia, H. *Eur. J. Inorg. Chem.* **2005**, 264.
- (32) Rhule, J. T.; Neiwert, W. A.; Hardcastle, K. I.; Do, B. T.; Hill, C. L. *J. Am. Chem. Soc.* **2001**, *123*, 12101.
- (33) Luan, G.; Li, Y.; Wang, S.; Wang, E.; Han, Z.; Hu, C.; Hu, N.; Jia, H. *J. Chem. Soc., Dalton Trans.* **2003**, 233.
- (34) Sheldrick, G. M. *Acta Crystallogr., Sect. A* **1998**, *46*, 467.
- (35) Sheldrick, G. M. *SHELXL-97. Program for Crystal structure analysis*; University of Göttingen: Germany, 1997.
- (36) Farrugia, L. J. *J. Appl. Crystallogr.* **1999**, *32*, 837.
- (37) Blessing, R. H. *Acta Crystallogr., Sect. A* **1995**, *51*, 33.
- (38) Coppens, P.; Leiserowitz, L.; Rabinovich, D. *Acta Crystallogr.* **1965**, *18*, 1035.
- (39) Bondi, A. *J. Phys. Chem.* **1964**, *68*, 441.

CG700736V